Arch. Metall. Mater. **66** (2021), 1, 241-248

DOI: 10.24425/amm.2021.134781

J. ADAMIEC[1*], N. KONIECZNA[1]

ASSESSMENT OF THE HOT CRACKING SUSCEPTIBILITY OF THE INCONEL 617 NICKEL-BASED ALLOY

Nickel alloys, despite their good strength properties at high temperature, are characterized by limited weldability due to their susceptibility to hot cracking. So far, theories describing the causes of hot cracking have focused on the presence of impurities in the form of sulphur and phosphorus. These elements form low-melting eutectic mixtures that cause discontinuities, most frequently along solid solution grain boundaries, under the influence of welding deformations. Progress in metallurgy has effectively reduced the presence of sulphur and phosphorus compounds in the material, however, the phenomenon of hot cracking continues to be the main problem during the welding of nickel-based alloys. It was determined that nickel-based alloys, including Inconel 617, show a tendency towards hot cracking within the high-temperature brittleness range (HTBR). There is no information on any structural changes occurring in the HTBR. Moreover, the literature indicates no correlations between material-related factors connected with structural changes and the amount of energy delivered into the material during welding.

This article presents identification of correlations between these factors contributes to the exploration of the mechanism of hot cracking in solid-solution strengthened alloys with an addition of cobalt (e.g. Inconel 617). The article was ended with development of hot cracking model for Ni-Cr-Mo-Co alloys.

Keywords: Inconel 617, nickel-based alloys, hot cracking, high-temperature brittleness range, weldability

1. Introduction

Modern materials for the power industry should display not only good mechanical properties, including high-temperature creep resistance and heat resistance, but also good technological properties. An important technological property is weldability. A major challenge for structural engineers, technologists, and welding engineers is the design and implementation of appropriate welding conditions for nickel-based alloys. According to literature data [1-3], the weldability of nickel-based alloys, i.e. their ability to form permanent joints, is classified as good. However, in practice, there are technological difficulties related to hot cracking. Hot cracks are unacceptable and disqualify welded joints from service [4,5].

So far, theories describing the causes of hot cracking have focused on the presence of impurities in the form of sulphur and phosphorus [3,6]. These elements form low-melting eutectic mixtures that cause discontinuities, most frequently along solid solution grain boundaries, under the influence of welding deformations. This results in hot cracking. Progress in metallurgy has effectively reduced the presence of sulphur and phosphorus compounds in the material, however, the phenomenon of hot cracking continues to be the main problem during the welding of nickel-based alloys [7-9].

In papers [6-11], it was determined that nickel-based alloys, including Inconel 617, show a tendency towards hot cracking within the high-temperature brittleness range (HTBR). The wider the HTBR, the higher the hot cracking susceptibility of the alloy. There is no precise definition of the high-temperature brittleness range. In the literature [3,6], the upper limit of the HTBR is defined as the nil strength temperature (NST) upon heating. Above this temperature, the material is unable to bear mechanical loads. The lower limit of the HTBR, in turn, is the ductility recovery temperature (DRT) upon cooling. Another definition was proposed by Prokhorov [11]. He set the upper limit of the HTBR as the liquidus temperature and located the lower limit near the solidus temperature [10-12].

Under crystallisation conditions within the high-temperature brittleness range, a material is affected by deformations related to material shrinkage, which may lead to the formation of microcrevices. Such microcrevices are not eliminated by an inflow of liquid metal as the network of dendrites prevents its access [4]. This type of hot cracking is referred to as brittle temperature range (BTR) cracking [6,13].

[1] SILESIAN UNIVERSITY OF TECHNOLOGY, FACULTY OF MATERIALS ENGINEERING AND METALLURGY, INSTITUTE OF MATERIALS ENGINEERING, 8 KRASIŃSKIEGO STR., 40-019 KATOWICE, POLAND

* Corresponding author: janusz.adamiec@polsl.pl

The authors of [13,14] also point out another type of hot cracking – ductility dip cracking (DDC). Such cracks occur at lower temperatures than BTR cracks. Discontinuities of this type result from reduced ductility of the material in the range between the solidus (T_s) and 0.5 T_s. A major decrease in the ductility of a nickel-based alloy is caused by deformations resulting from progressing crystallisation. The main mechanism of DDC cracking is the partial melting of carbides in the material [11-15]. Fig. 1 shows the formation of DDC and BTR hot cracks depending on the temperature and ductility [12].

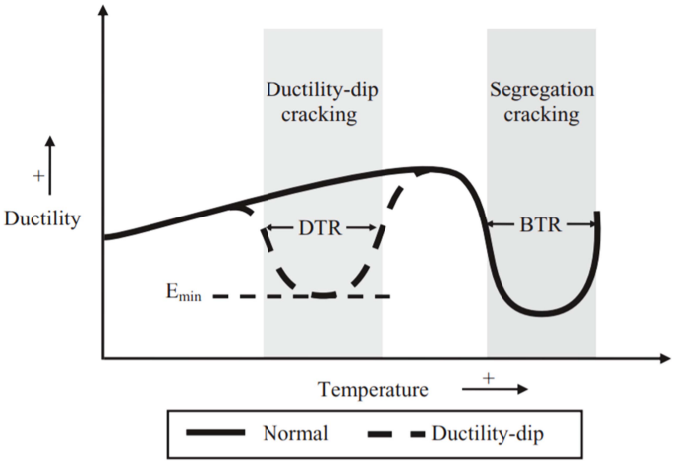

Fig. 1. Formation of DDC and BTR hot cracks with reduced ductility, E_{min} – minimum ductility during decrease of crystallization temperature [12]

Hot cracking susceptibility is also affected by the structure forming during crystallisation, including the supercooling degree (ΔT), understood as the difference between the theoretical and actual crystallisation temperature. A low supercooling degree involves a risk of the formation of column-shaped crystallites, which increases the hot cracking susceptibility of a material. When the supercooling degree is high, hot cracking susceptibility is limited due to the formation of a dendritic structure [3].

The literature [1-4] describes only the general hot cracking mechanism in nickel-based alloys. There is no information on any structural changes occurring in the HTBR. Moreover, the literature indicates no correlations between material-related factors connected with structural changes and the amount of energy delivered into the material during welding. The identification of correlations between these factors contributes to the exploration of the mechanism of hot cracking in solid-solution strengthened alloys with an addition of cobalt (e.g. Inconel 617). It is necessary to assess the weldability of Inconel 617, understood as the susceptibility of this alloy to hot cracking.

Thus, the aim of work is described the phenomena occurring in the high temperature brittleness range during the welding of Inconel 617 alloy and determine the hot cracking mechanism for the examined alloy.

2. Description of the material

Inconel 617 (UNS N06617 according to ASME SB-168:2013) rods having a diameter of 6 mm and 3 and 5 mm thick plates manufactured by TyssenKrupp VDM were used for the tests. The chemical composition (Table 1) was verified by X-ray fluorescence (XRF) using a Niton XL2 spectrometer. The XRF results is presented in Table 1.

Based on the results of the measurement of the percentage of elements in Inconel 617, it was determined that the material tested met the requirements of ASME SB-168:2013 and that the element contents set out in the material specifications fell within the acceptable limits. Moreover, small amounts of niobium were found in the material(below 0.2%). Niobium is a strong carbide former; it forms fine-sized, compound, strengthening carbonitrides [16,17].

Following rolling, all the plates were heat-treated (solution treatment). The 3 mm thick plates were annealed at 1177°C for 9 minutes and then cooled in air for 144 s, whereas the 5 mm thick plate was annealed at 1160°C for 16 minutes and cooled in water [18-20]. This heat treatment is recommended for the solid-solution strengthening of the alloy.

Examples of the alloy's mechanical properties at ambient temperature according to ASME SB-168:2013 and according to the manufacturer's specifications are presented in Table 2. The values of tensile strength (R_m), the minimum yield strength ($R_{0.2}$), and elongation (A) set out in the specifications for all plates fall within the ranges of values laid down by ASME SB-168:2013 [18-21].

Metallographic examinations carried out under a light microscope confirmed the grain size evaluation results obtained by the manufacturer and presented in appropriate specifications. A one-phase granular structure with visible twins and fine carbides was observed in the samples examined (Fig. 2).

According to the specifications for the 5 mm thick plate (specifications No. 95198/1, heat 331145), the average grain diameter was 74 μm, which meets the requirements for class 4.5 according to ASTM E112 (Fig. 2a,b). Based on the metallographic examinations, the EDS microanalysis of the chemical composition, the XRD phase analysis, and the identification of the phases revealed in the structure by means of electron diffrac-

TABLE 1

The chemical composition of Inconel 617 alloy according to XRF results and ASME SB-168:2013 standard

IN617	Cr	Co	Mo	Al	Fe	Mn	Si	Ti	Cu	S	P	B	C
XRF	20.47	12.11	9.87	—	0.89	—	—	0.28	—	—	—	—	—
ASME SB-168:2013	20-24	10-15	8-10	0.8-1.5	max 3.0	max 1.0	max 1.0	max 0.6	max 0.5	max 0.015	—	max 0.006	0.05-0.15

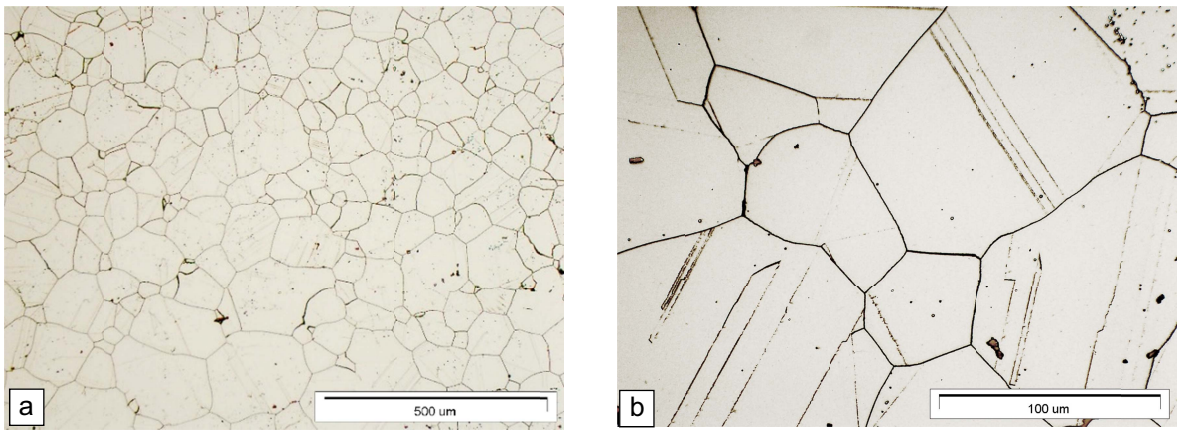

Fig. 2. Microstructure of Inconel 617, light microscope (LM): a) structure of the 5 mm thick plate, magn. 100×, b) structure of the 5 mm thick plate, magn. 500×

TABLE 2

Mechanical properties of Inconel 617 [18]

Heat: L40252 Specification No.: 27424	Mechanical properties according to ASME SB-168:2013		
	R_m, MPa	$R_{p0.2}$, MPa	A, %
	min. 655	min. 240	min. 25
	Mechanical properties of Inconel 617 according to the specifications		
	R_m, MPa	$R_{p0.2}$, MPa	A, %
	851	401	63

tion, it was determined that the rolled Inconel 617 plates were built of polygonal γ phase grains with sparse plate precipitates of $M_{23}C_6$ carbides along grain boundaries and globular carbides inside grains. Sparse γ/γ' eutectic mixture areas and titanium nitrides were also identified in the structure.

3. Analysis and discussion of the obtained results

3.1. Determination of the critical HTBR temperatures for Inconel 617

The purpose of the tests was to determine the characteristic temperatures for the crystallisation process of Inconel 617. The tests were performed on a Gleeble 3800 thermal-mechanical simulator.

The tests enabled the determination of the:

- Nil Strength Temperature (NST) – the temperature upon heating at which the material's strength goes towards zero;
- Nil Ductility Temperature (NDT) – the temperature upon heating at which the material's ductility goes towards zero;
- Ductility Recovery Temperature (DRT) – the temperature upon cooling at which the material becomes deformable;
- High Temperature Brittleness Range (HTBR) – the range of temperatures within which the material is susceptible to hot cracking;
- hot cracking susceptibility index: $R_f = (T_l - \text{NDT})/\text{NDT}$, T_l – liquidus.

The results obtained enabled the determination of the influence of structural factors on the hot cracking susceptibility of Inconel 617.

3.2. Characteristic temperatures during the crystallisation of Inconel 617

Characteristic temperatures for the crystallisation and melting of Inconel 617, i.e. the temperatures of the beginning (liquidus – T_l) and end (solidus – T_s) of crystallisation, were determined by means of differential thermal analysis (DTA). The DTA was performed using a Setaram SETSYS thermal analyser. A TG-DTA head was used to record temperatures at which transformations related to the melting and crystallisation of the alloy occur both upon heating and upon cooling. A type S (Pt-Rh/Pt-Rh 10%) thermocouple was used for the DTA. The samples were heated at a rate of 10°C/min up to the temperature of 1500°C in an argon atmosphere with a flow of 1.35 l/h. A DTA curve for heating is shown in Fig. 3, whereas Fig. 4 presents a DTA curve for cooling. The temperatures of the beginning and end of the transformation were determined by the one set point method. The results of the calculations are set out in Table 3.

An analysis of the DTA curves for heating indicates that the liquid phase appears at 1343°C, whereas at 1420°C the alloy becomes completely liquid (Fig. 3, Table 3). The temperature at which the first solid phase crystals start to appear upon cooling (T_L) was found to be 1390°C. The adopted crystallisation temperature upon cooling (T_{peak}) was 1380°C and the solidus (T_s) was 1279°C (Fig. 4, Table 3).

In the Inconel 617 weldability tests, i.e. the welded joint hot cracking susceptibility tests, the solidus and liquidus temperatures determined upon cooling were adopted due to the weld crystallisation process during the welded joint's cooling. On this basis, it was determined that the range between the solidus and the liquidus upon cooling was 111°C.

The liquidus and solidus temperatures determined for the alloy concerned were used in tests on a Gleeble 3800 thermal-mechanical simulator for the purpose of determining the hot cracking susceptibility index (R_f) and the HTBR of Inconel 617.

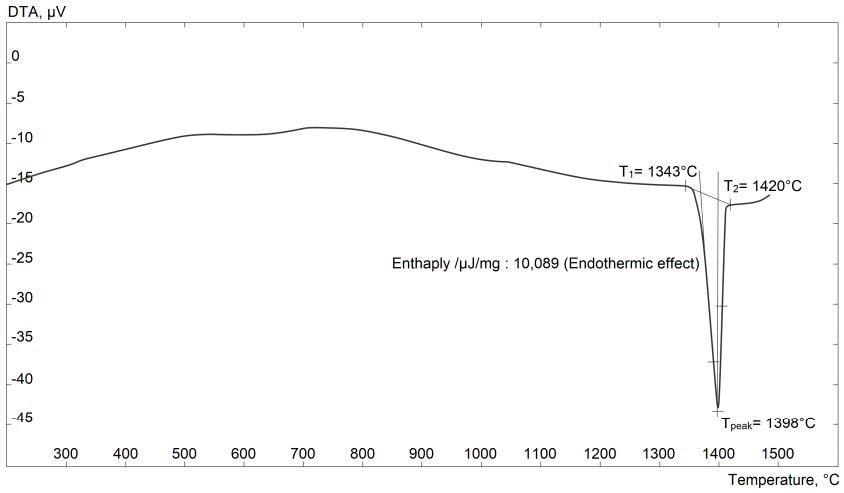

Fig. 3. DTA curve for the heating of Inconel 617

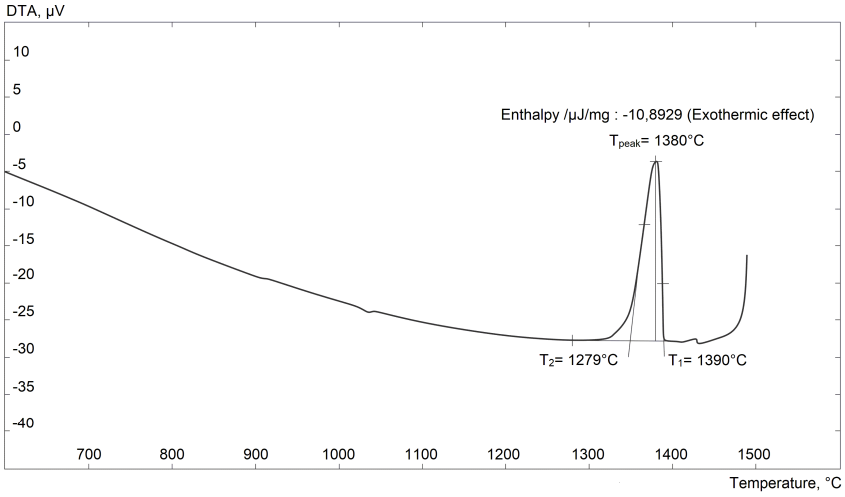

Fig. 4. DTA curve for the cooling of Inconel 617

TABLE 3

Characteristic temperatures of Inconel 617

Temperature at which the liquid phase starts to appear upon heating, T_1, °C	Temperature of the beginning of melting upon heating, T_{peak}, °C	Temperature of the end of melting upon heating, T_2, °C	**Liquidus temperature** Temperature at which the first solid phase crystals start to appear upon cooling, T_L, °C	Crystallisation temperature upon cooling, T_{peak}, °C	**Solidus temperature** End of crystallisation upon cooling, T_2, °C
1343	1394	1420	**1390**	1380	**1279**

3.3. The nil strength temperature (NST) of Inconel 617

In order to determine the NST for Inconel 617, tests on cylindrical samples measuring Ø 6 × 90 mm were conducted on a Gleeble 3800 simulator. Type S thermocouples were applied to the samples, which were subsequently mounted in special copper grips in the testing chamber, at a distance of 52.4 mm from each other. After air was pumped out of the chamber, it was filled with argon (up to 0.4 hPa). Each sample received an initial load (0.6-0.7 kN) that was sustained until the end of the test. The samples were heated at a rate of 20°C/s up to 1200°C and then at a rate of 1°C/s up to the fracture temperature. The NST was determined as the average temperature at which cracks appeared in five samples. The NST measurement results are presented in Table 4. Fig. 5 shows the fracture surface and the crack area microstructure revealed on a section perpendicular to the fracture surface.

An analysis of the Gleeble 3800 simulator test results showed that at the NST = 1330 °C, grain boundaries were subject to partial melting across an approx. 200 µm wide area (Fig. 5a). This results in discontinuities in the material, perpendicularly to the sample axis, as a result of the loss of cohesion by the liquid between grains (Fig. 5). This was also confirmed by fractographic examinations. An analysis of the fracture surface revealed a smooth grain surface with visible partially melted boundaries of the polygonal grains of the γ matrix (Fig. 5b).

TABLE 4

The nil strength temperature (NST) upon heating of Inconel 617

NST, °C	1335
	1333
	1329
	1327
	1325
Average NST, °C	1330 ± 4

3.4. The nil ductility temperature (NDT), the ductility recovery temperature (DRT), and the hot cracking susceptibility index (R_f)

The NDT and the DRT were determined for Inconel 617 in order to assess the width of the HTBR and to determine the influence of the structure on the hot cracking mechanism. The temperature at which a sample's reduction in area is less than 5% was adopted as the NDT and a reduction in area of more than 5% was adopted as the DRT [22].

The tests were conducted using a Gleeble 3800 simulator. Cylindrical samples measuring Ø 6 × 120 mm were mounted in copper grips in a protective argon atmosphere. In order to identify the NDT, the samples were heated to a pre-defined temperature within the HTBR, then annealed for 10 s, and then stretched at a defined fixed rate (20 mm/s). The DRT was determined as the temperature at which a sample's reduction in area was less than 5%. The samples were cooled down from a temperature close to the NST to a pre-defined value and then stretched at a fixed rate. A strain rate of 20 mm/s was adopted both for the NDT and the DRT tests. Changes in the samples' reduction in area as a function of temperature upon heating (determination of the NDT) and upon cooling (determination of the DRT) are shown in Fig. 6. The determined NDT and DRT and the calculated hot cracking susceptibility index R_f are set out in Table 5. The results obtained enabled the determination of the width of the HTBR, which was defined as the difference between the NST and the DRT (Table 5).

TABLE 5

NDT and DRT determined on a Gleeble 3800 simulator, the value of R_f, and the HTBR of Inconel 617

NDT, °C	DRT, °C	R_f	HTBR, °C	HTBR width, °C
1230±4	1175±2	0.13	1330 ÷ 1175	155

The tests were complemented by microscope observations of the structure in the crack area. Examples of results of these examinations are shown in Fig. 7 for the samples subjected to the NDT tests and in Fig. 8 for the samples subjected to the DRT tests.

Based on the results obtained it was established that upon heating, Inconel 617 lost ductility (reduction in area below 5%) at 1230°C (Table 5). This temperature was adopted as the NDT (Fig. 6). Upon cooling, in turn, at 1175°C, the material recovered its ductile properties (reduction in area above 5%). This value was adopted as the DRT for Inconel 617 (Fig. 6, Table 5).

4. Analysis of the results

The results obtained enabled determining the width of the HTBR as the difference between the NST upon heating – 1330°C – and the DRT upon cooling, i.e. 1175°C (Table 5). The width of the HTBR is 155°C (Fig. 6). Inconel 617 is susceptible to hot cracking within this temperature range. The value of the calculated R_f index, understood as the ratio of the difference between the liquidus and the NDT to the NDT, amounting to 0.13, indicates that the hot cracking susceptibility of Inconel 617 is at a level similar to that of the entire group of Ni-Cr-Mo nickel-based alloys (Table 5) [6, 23-25].

An analysis of the fracture surface of Inconel 617 upon heating (Fig. 7) (NDT determination) indicated that the material lost cohesion as a result of the partial melting of grain boundaries and the rupture of the thin liquid film along grain boundaries (Fig. 7a). This was confirmed by the results of fractographic examinations (Fig. 7b). On the fracture surface, polygonal grains with intergranular cracks were observed, formed as a result of the

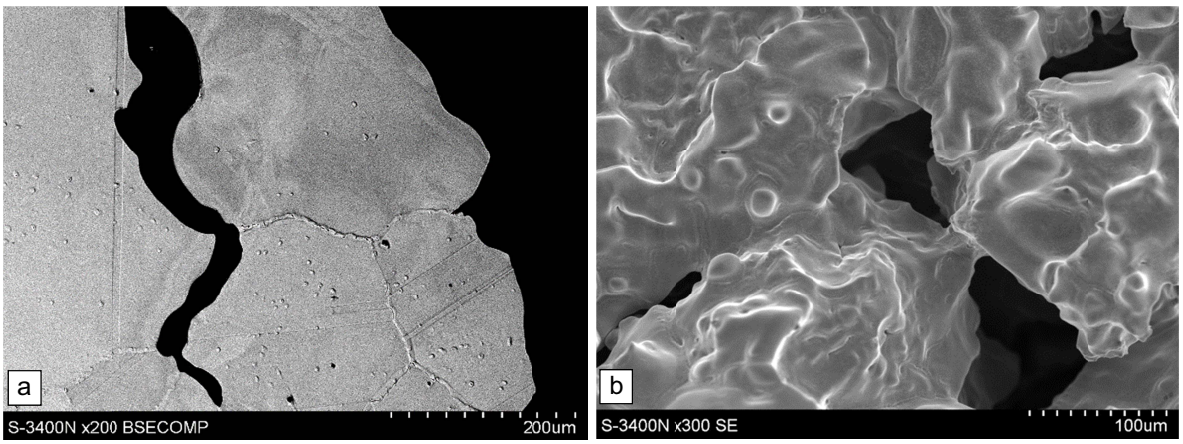

Fig. 5. Structure of the fracture area in Inconel 617 after the test aimed at determining the NST, a) microstructure of the area perpendicular to the fracture, intergranular fracture, LM, b) fracture surface, partial melting of γ phase grains, SE image

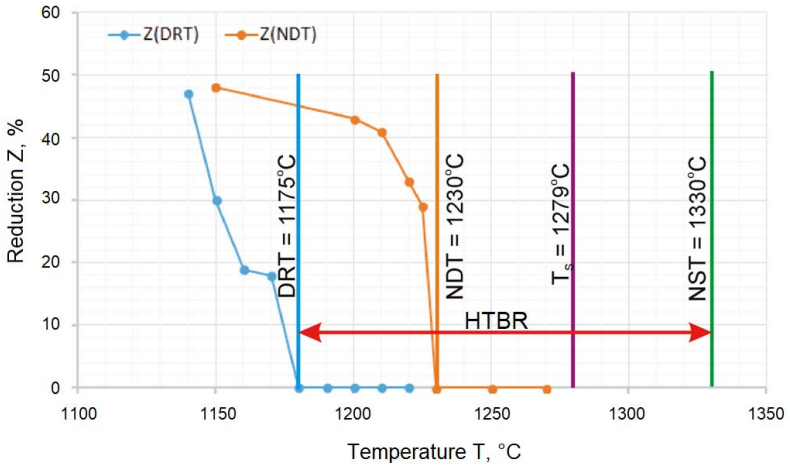

Fig. 6. Reduction in area in Inconel 617 as a function of temperature upon heating (NDT determination) and upon cooling (DRT determination)

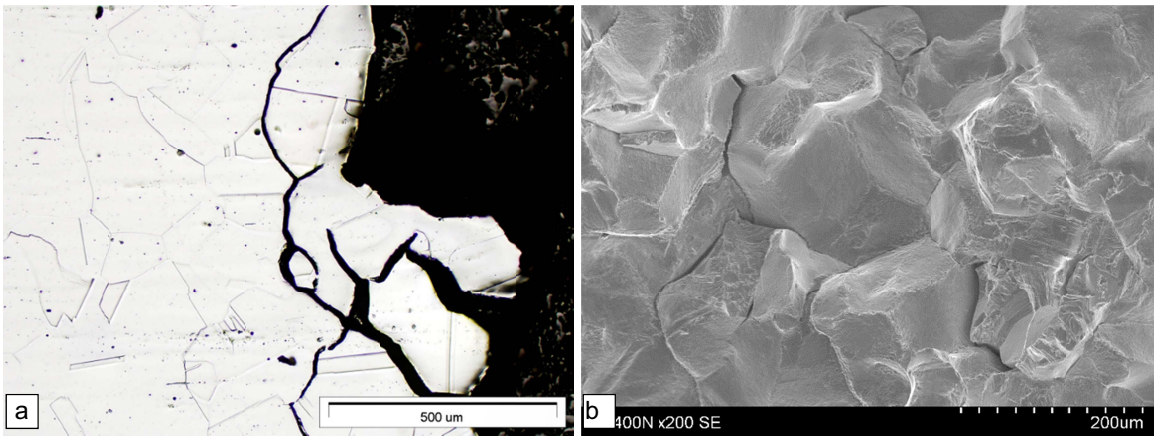

Fig. 7. Structure of a crack area in Inconel 617 after the NDT test, test temperature 1300°C: a) microstructure of the area perpendicular to the fracture surface, visible local partial melting of γ matrix grains, LM, b) fracture surface, visible partial melting of γ matrix grains with a network of cracks propagating from the fracture surface along grain boundaries and broken bridges between grains, SE image

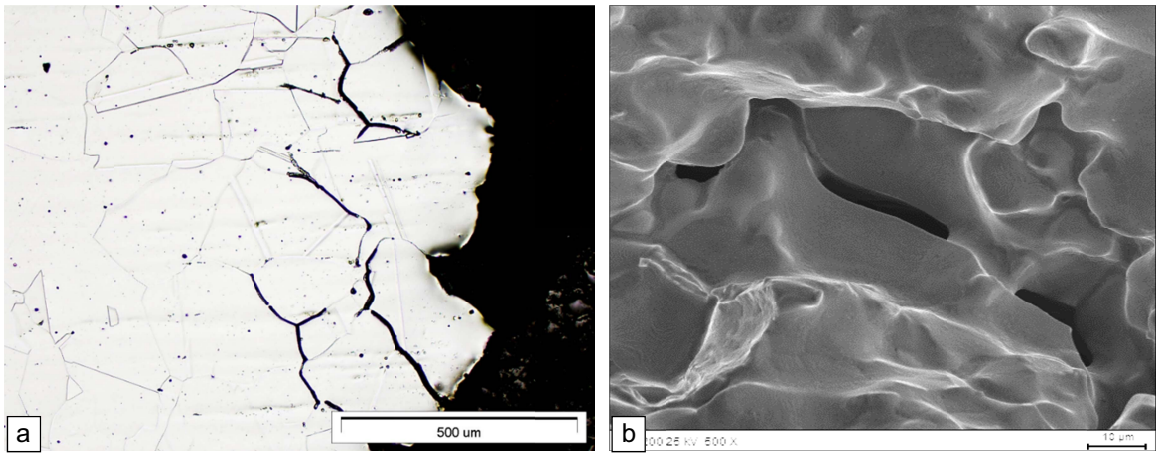

Fig. 8. Structure of a crack area in Inconel 617 after the DRT test, test temperature 1220°C: a) microstructure of the area perpendicular to the fracture surface, local partial melting of γ matrix grains, LM, b) fracture surface, visible partial melting of matrix grains with a network of intergranular cracks propagating from the fracture surface and bridges between grains, SE image

loss of cohesion by the liquid, as well as transgranular cracks, being the effect of the rupture of "bridges" in the material in the solid state (Fig. 7b). This cracking mechanism was also confirmed by the results of observations under a light microscope (Fig. 7a). A network of cracks was observed, mainly along grain boundaries in a zone that was approx. 400 μm wide.

Examinations of the structure of Inconel 617 after the DRT tests revealed a network of cracks along γ matrix grain bounda-

ries with numerous cracks propagating from the fracture surface (Fig. 8a). The alloy loses cohesion as a result of the coalescence of cracks along grain boundaries, which leads to a network of cracks that grows into a main crack. This is confirmed by fractographic examinations of the fracture surface. Polygonal γ matrix grains with numerous cracks propagating from the fracture surface along grain boundaries were observed on the fracture surface (Fig. 8b). Moreover, bridges between particular grains, characteristic of hot cracking within the HTBR, were observed. The bridges formed from the material that was not melted and from crystallised intergranular liquid (Fig. 8b).

As part of the HTBR tests of Inconel 617, the solidus temperature (T_s = 1279°C) and the liquidus temperature (T_L = 1390°C) were determined by DTA (Table 2). An analysis of the literature data indicates that the determined temperatures fall within the solidus and liquidus ranges specified for Inconel 617, which also corresponds with the material specification provided by the manufacturer [18-21]. The range of temperatures between the liquidus and the solidus is 111°C. An analysis of the results obtained in the NST tests showed that the nil strength temperature of the alloy concerned was 1330°C (Table 4). It was found that the main cohesion loss mechanism at this temperature is the partial melting of the grain boundaries and the occurrence of discontinuities in the intercrystalline liquid (Fig. 5).

Upon heating, Inconel 617 loses ductility at 1230°C (the NDT) (Table 5). Upon cooling, the alloy recovers its ductile properties at 1175°C (the DRT) (Table 5).

The HTBR determined for Inconel 617 is 155°C (Fig. 6) and falls between 1175°C (the DRT) and 1330°C (the NST). Within this range, Inconel 617 is susceptible to hot cracking, which is also confirmed by the calculated hot cracking susceptibility index R_f, which is 0.13 (Table 5).

The results of the HTBR tests, complemented by fractographic examinations of the surfaces of the hot cracks revealed during the melting of the test plates, enabled describing the cracking mechanism and the particular crack propagation phases (Fig. 9).

Fractographic examinations of the crack surface indicate that hot cracking in Inconel 617 occurs along partially melted dendrite boundaries (Fig. 9). The main mechanism of hot cracking in the alloy is the loss of continuity by the liquid at partially melted dendrites, which undergo deformation during the

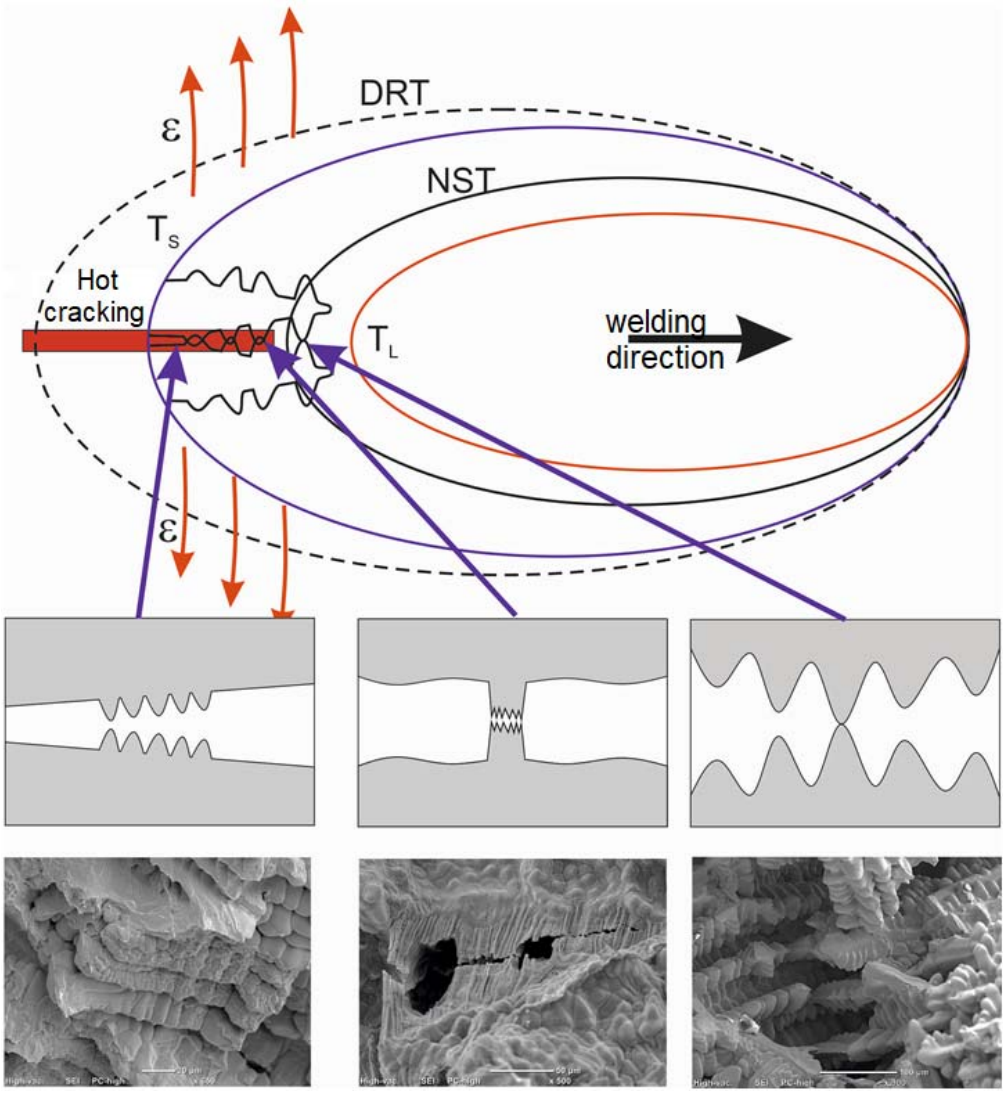

Fig. 9. Diagram of the hot cracking mechanism in Inconel 617 in the HTBR during the welding of TIG method

crystallisation. Cracks initiate in the partially melted area. The progressing crystallisation of Inconel 617 cuts off the inflow of liquid metal, causing plastic deformation of dendrites and thus the rupture of bridges between them. This hot cracking process is characteristic of the range of temperatures within which the material is recovering its ductility (DRT). A larger number of bridges between dendrites were found near the end of the weld pool and in the already-crystallised area, which is related to the heat cycle of welding and the movement of the heat source (Fig. 9).

5. Summary

The following conclusions were formulated based on the tests and examinations conducted and the analysis of their results:

1. The main hot cracking mechanism in Inconel 617 is the loss of continuity by the liquid at partially melted dendrites in the thin liquid layer in the partially melted area. During crystallisation, the dendrites are additionally subject to tensile stresses. Deformation causes the rupture of bridges between dendrites and crack propagation along crystallite boundaries. Hot cracks form as a result of a limited inflow of liquid metal to partially melted areas. Adjoining dendrites form a dense solid body network, limiting the flow of liquid metal, which results in the loss of cohesion by the interdendritic liquid film. Hot cracking occurs in the liquid-solid state in the high-temperature brittleness range.
2. The width of the HTBR for Inconel 617 is 155°C. The HTBR falls between the nil strength temperature upon heating (NDT = 1330°C) and the ductility recovery temperature upon cooling (DRT = 1175°C). Inconel 617 is susceptible to hot cracking within this temperature range. The hot cracking susceptibility index R_f was determined to be 0.13.

REFERENCES

[1] N.L. Richards, M.C. Chaturvedi, Effect of minor elements on weldability of nickel base superalloys, International Materials Reviews **45**, 109-129 (2000).

[2] M.B. Henderson, D. Arrell, R. Larsson, M. Heobel, G. Marchant, Nickel based superalloy welding practices for industrial gas turbine applications, Science and Technology of Welding and Joining **9**, 13-21 (2004).

[3] E. Tasak, Metalurgia spawania, Wydawnictwo JAK, Kraków (2008).

[4] J.A. Siefert, J.P. Shingledecker, J.N. DuPont, S.A. David, Weldability and weld performance of candidate nickel based superalloys for advanced ultrasuperitical fossil power plants Part II: weldability and cross-weld creep performance, Science and Technology of Welding and Joining **21**, 397-428 (2016).

[5] T. Chu, H. Xu, Z. Li, F. Lu, Investigation of intrinsic correlation between microstructure evolution and mechanical properties for nickel-based weld metal, Materials & Design **165**, 107595 (2019).

[6] T. Böllinghaus, H. Herold, C.E. Cross, J.C, Lippold, Hot Cracking Phenomena in Welds II, Springer, Berlin (2008).

[7] G.A. Young, T.E. Capobianco, M.A. Penik, B.W. Morris, J.J. McGee, The mechanism of Ductility Dip Cracking in Nickel-Chromium Alloys, Supplement to the Welding Journal **87**, 31-43 (2008).

[8] K. Mageshkumar, N. Arivazhagan, P. Kuppan, Studies on the effect of filler wires on micro level segregation of alloying elements in the alloy 617 weld fusion zone, Materials Research Express **11**, 116579 (2019).

[9] N.E. Nissley, M.G. Collins, G. Guaytima, J.C. Lippold, Development of the Strain-to-Fracture Test for Evaluating Ductility-Dip Cracking in Austenitic Stainless Steels and Ni-Base Alloys. Welding Research **46**, 32-40 (2003).

[10] N.E. Nissley, J.C. Lippold, Ductility-Dip Cracking Susceptiblity of Nickel-Based Weld Metals: Part 2 – Microstructural Characterization, Welding Research **88**, 131-140 (2009).

[11] N.N. Prokhorov, Russian Castings Production, Moscow, (1962).

[12] J.M. Kikel, D.M. Parker, Ductility Dip Cracking Susceptibility of Inconel Fill Metal 52 and Inconel Alloy 690, International Conference on trends in welding research; Pine Mountain, United States, Report number MAO-T-98-0233 (1998).

[13] A.J. Ramirez, J.W. Sowards, J.C. Lippold, Improving the ductility-dip cracking resistance of Ni-base alloys, Journal of Materials Processing Technology **179**, 212-218 (2006).

[14] M.G. Collins, J.C. Lippold, An investigation of ductility-dip cracking in Ni-base filler metals-Part 1, Welding Journal **82**, 288-295 (2003).

[15] H.K. D.H. Bhadeshia, Nickel Based Superalloy, University of Cambridge, http://www.phase-trans.msm.cam.ac.uk/2003/Superalloys/super-alloys.html (accessed 20 July 2019)

[16] C. Soares, Gas Turbines: A handbook of air, land and sea applications, Elsevier Science, Oxford (2015).

[17] J.R. Davis, Nickel, Cobalt, and Their Alloys, ASM International, United States of America: (2000).

[18] Materials specification, number 27424.

[19] Materials specification, number 104727/0.

[20] Materials specification, number 95198/1.

[21] ASME SB-168:2013 standard, Specification for nickel-chromium-iron alloys (UNS N06600, N06601, N06603, N06690, N06693, N06025, and N06045) and nickel-chromium-cobalt-molybdenum alloy (UNS N06617) plate, sheet and strip, w ASME Boiler and Pressure Vessel Code: II Materials Part B – Nonferrous Material Specifications, 228-241 (2013).

[22] Gleeble 3800 Applications, Welding Process Simulation, New York, 55-62 (2000).

[23] A. Turowska, J. Adamiec, Zakres kruchości wysokotemperaturowej złączy spawanych stopu Inconel 625. Przegląd Spawalnictwa **87**, 104-107 (2015).

[24] J. DuPont, J. Lippold, S. Kiser, Welding metallurgy and weldability of nickel-base alloys, John Wiley & Sons, New York (2009).

[25] P.E.A. Turchi, L. Kaufman, Z.K. Liu, Modeling of Ni-Cr-Mo based alloys: Part I – phase stability. Calphad **30**, 70-87 (2006).